Synthesis and Photovoltaic Performances of Benzo[1,2-b:4,5-b′] dithiophene-*alt*-2,3-diphenylquinoxaline Copolymers Pending Functional Groups in Phenyl Rings

Hua Tan, Xianping Deng, Junting Yu, Jianhua Chen, Kaixuan Nie,
Ying Huang, Yu Liu, Yafei Wang, Meixiang Zhu, Weiguo Zhu

College of Chemistry, Xiangtan University, Key Lab of Environment-Friendly Chemistry and Application in Ministry of Education, Xiangtan 411105, China
Correspondence to: Dr. W. Zhu (E-mail: zhuwg18@126.com)

Received 3 August 2012; accepted 5 November 2012; published online 4 December 2012
DOI: 10.1002/pola.26477

ABSTRACT: Two donor/acceptor (D/A)-based benzo[1,2-b:4,5-b′]dithiophene-*alt*-2,3-biphenyl quinoxaline copolymers of **P**1 and **P**2 were synthesized pending different functional groups (thiophene or triphenylamine) in the 4-positions of phenyl rings. Their thermal, photophysical, electrochemical, and photovoltaic properties, as well as morphology of their blending films were investigated. The poly(4,8-bis((2-ethyl-hexyl)oxy)benzo[1,2-b:4,5-b′] dithiophene)-*alt*-(2,3-bis(4′-bis(N,N-bis(4-(octyloxy) phenylamino)-1,1′-biphen-4-yl)quinoxaline) (**P**2) exhibited better photovoltaic performance than poly(4,8-bis((2-ethylhexyl)oxy)benzo[1,2-b:4,5-b′] dithiophene)-*alt*-(2,3-bis(4-(5-octylthiophen-2-yl)phenyl)quinoxaline) (**P**1) in the bulk-heterojunction polymer solar cells with a configuration of ITO/PEDOT:PSS/polymers: [6,6]-phenyl-C_{71}-butyric acid methyl ester ($PC_{71}BM$)/LiF/Al. A power conversion efficiency of 3.43%, an open-circuit voltage of 0.80 V, and a short-circuit current of 9.20 mA cm^{-2} were achieved in the **P**2-based cell under the illumination of AM 1.5, 100 mW cm^{-2}. Importantly, this power conversion efficiency level is 2.29 times higher than that in the **P**1-based cell. Our work indicated that incorporating triphenylamine pendant in the D/A-based polymers can greatly improved the photovoltaic properties for its resulting polymers.© 2012 Wiley Periodicals, Inc. J. Polym. Sci., Part A: Polym. Chem. **2013**, *51*, 1051–1057

KEYWORDS: benzo[1,2-b:4,5-b′]dithiophene; quinoxaline; D-A copolymer; polymer solar cells; bulk heterojunction

INTRODUCTION Polymeric solar cells (PSCs) have attracted considerable attention in recent years due to their potentials of low-cost manufacture, easy processability over large area via printing or roll-to-roll coating technologies, and favorable compatibility with flexible substrates. In these developed PSCs, the devices with bulk heterojunction (BHJ) structure exhibited some encouraged photovoltaic performance, where an electron-rich polymer and an electron-deficient fullerene were blended in the photoactive layer.[1–8] As the BHJ structure not only provides a large-area donor-acceptor interface for charge separation but also can form a discontinuous interpenetrating network for charge transport, the BHJ-based PSCs are available to present high power conversion efficiency (PCE). Up to now, the highest PCE of 9.2% was reported by Cao and coworkers in this type of PSCs.[9]

However, the photovoltaic levels of these reported copolymers in the devices have not met commercial requirements for application. The unideal results were considered to be mainly related to the spectral mismatch between the copolymer's absorption and the terrestrial solar spectra.[10,11] In order to enhance the absorption to sunlight, the ideal polymers need to harvest more additional solar photons at longer wavelengths, particularly in the near-IR region, and exhibit much broader spectra. Therefore, one feasible approach was to design various D-A copolymers with electron-rich donor (D) unit and electron-deficient acceptor (A) unit. Owing to an additional intramolecular charge transfer from the D unit to the A unit, these D-A copolymers presented wider absorption spectral bands. By tuning the structures of D and A units, some D-A copolymers showed improved photovoltaic properties with PCE as high as 3–8%.[12–16]

Quinoxaline is a typical electron-deficient conjugated unit due to the strong electronegativity of its two nitrogen atoms and usually employed to construct conjugated polymers with D-A backbone in the main chain.[17–20] For example, Yang et al.[21] reported a series of soluble thiophene-*alt*-quinoxaline D-A polymers pending a hole-transporting carbazole moiety as a side chain and obtained the PSCs with a PCE of 0.40%. Lee et al. presented a series of dioctyloxybenzo[1,2-b;3,4-b′]dithiophene-*alt*-bis(2-thienyl)-2,3- diphenylbenzo[g]quinoxaline low

Additional supporting information may be found on the online version of this article.

TABLE 1 Polymerization Results and Thermal and Optical Properties of **P**1 and **P**2

Polymer	M_n[a] ($\times 10^4$)	M_w[a] ($\times 10^4$)	PDI[a]	T_d[b] (°C)	Absorption[c] (λ_{max}/nm) (ε_{max}/dm^3 mol^{-1} cm^{-1})
P1	1.61	3.29	2.04	356	300 (2.5×10^6), 385 (2.4×10^6), 586 (1.2×10^6)
P2	2.73	5.34	1.96	363	299 (3.6×10^6), 402 (3.2×10^6), 612 (1.3×10^6)

[a] M_n,M_w, and PDI of the polymers were determined by GPC using polystyrene standards.

[b] T_d were measured by TGA at a temperature of 5% weight loss for the polymers.

[c] Measured in the DCM at 298 K.

bandgap copolymers. By attaching methoxy or fluorine groups into the phenyl rings, this kind of copolymers exhibited a maximum PCE of 1.42% with an open-circuit voltage (V_{oc}) of 0.8 V, a short-circuit current (J_{sc}) of 5.73 mA cm^{-2}, and a fill factor (*FF*) of 30.9% under illumination of AM 1.5, 100 mW cm^{-2}.[22] Recently, Hou and coworkers designed a kind of dioctyloxybenzo[1,2-b;3,4-b']dithiophene-*alt*-bis(2-thienyl)-2,3-diphenylquinoxaline conjugated polymers and exhibited a PSC with a PCE of 3.06%. By further applying two-dimensional conjugated benzo-[1,2-b:4,5-b']dithiophene in the above conjugated polymers, his group achieved an improved PSC with a PCE as high as 5.0%.[23] Meanwhile, Zou et al. developed another type of indacenodithiophene-*alt*-quinoxaline copolymers and obtained inverted PSCs with a maximum PCE of 6.38%. To my best knowledge, this is the highest PCE value reported in PSCs using quinoxaline-based conjugated polymer as donors up to now.[24]

In this article, in order to explore the effect of the pending functional groups on the photovoltaic performance of the quinoxaline-based conjugated polymers, two D-A-based benzo[1,2-b:4,5-b′]dithiophen-*alt*-2,3-biphenyl quinoxaline copolymers of **P**1 and **P**2 were designed and synthesized pending the functional groups of thiophene or triphenylamine in the 4-positions of the phenyl rings. Here, the **P**1 is poly(4,8-bis ((2-ethylhexyl)oxy) benzo[1,2-b:4,5-b']dithiophene)-*alt*-(2,3-bis(4-(5-octylthiophen-2-yl)phenyl)quinoxaline) and the **P**2 is poly(4,8-bis((2-ethylhexyl)oxy)benzo[1,2-b:4,5-b']dithiophene)-*alt*-(2,3-bis(4'-bis (*N*,*N*-bis(4-(octyloxy)phenylamino)-1,1'-biphen-4-yl)quinoxaline). Their photophysical, electrochemical, and photovoltaic properties were studied. The best performances were observed in the BHJ PSC devices using **P**2 copolymer with pendent triphenylamine unit as the active layer. A maximum PCE of 3.43% with a V_{oc} of 0.80 V, a J_{sc} of 9.20 mA cm^{-2} and a *FF* of 47.0% was achieved under the illumination of AM 1.5, 100 mW cm^{-2}. Our work indicated that photovoltaic properties of the D-A quinoxaline-based copolymers can be improved by attaching the functional group of triphenylamine.

RESULTS AND DISCUSSION

Synthesis and Characterization of the Polymers

4,7-dibromo-2,1,3-benzothiadiazole was reduced with zinc in acetic acid to afford 1,4-bibromo-2,3-diaminobenzene, condensation of 1,4-bibromo-2,3-diaminobenzene with diketone 2 or 4 to obtain the M2 and M3, respectively. The M2 and M3 were subsequently copolymerized with 2,6-bis(trimethyltin)-4,8-bis(2-ethyl-hexyloxy)-benzo[1,2-b:4,5-b']dithiophene to afford P1 and P2, respectively. Because of the side chains, the P1 and P2 showed good solubility in common organic solvents, such as chlorobenzene, *o*-dichlorobenzene, and dichlomethane (DCM).

Thermal Stability

The thermal property of **P**1 and **P**2 was investigated by thermogravimetric analysis (TGA). Figure S2 shows the TGA curves of two copolymers. These data are summarized in Table 1. The degradation temperatures (T_d) of 356 °C and 363 °C are observed for **P**1 and **P**2 with 5% weight loss, respectively. Obviously, the **P**2 polymer with pendent triphenylamine group exhibited better thermal property than the **P**1 polymer with pendent thiophene group. It means that introducing the electron-donor triphenylamine group into the side chain of quinoxaline unit has a positive effect on the thermal stability of its resultant copolymer.

Dispersible Property

In general, photovoltaic properties of PSCs are greatly affected by the surface morphology of the photoactive layer. Good morphology is available to form excellent interpenetrating networks in the active layer and further facilitate charge separation and transportion of photogenerated excitons, finally increase the *FF* level of the devices. Therefore, it is necessary to investigate dispersible property of the polymer donor in the PC$_{71}$BM acceptor. Based on this consideration, the typical blend films of **P**1 and **P**2 in PC$_{71}$BM were made, in which the weight ratio of polymer and PC$_{71}$BM was of 1:3. Their surface morphologies were recorded by atomic force microscopy (AFM) in a tapping mode as shown in Figure 2. The roughness of 0.363 nm and 0.639 nm for the **P**1:PC$_{71}$BM and **P**2:PC$_{71}$BM blend films are observed, respectively. Compared to the reported results, both **P**1 and **P**2 polymers have a good dispersibility in the PC$_{71}$BM matrix.

Optical Property

The UV-Vis absorption spectra of **P**1 and **P**2 in dilute DCM and their neat films are shown in Figure 1. Their UV-Vis absorption data are also summarized in Table 1. Similar absorption spectra with two π-π* transitions of the D and A units in the 260–480 nm range and an intramolecular charge transfer transition in the 500–750 nm range are exhibited for the **P**1 and **P**2 polymers. However, the absorption intensity and peak site have a significant difference with various units introduced in the 2,3-positions of quinoxaline group. The maximum absorption peak located at 612 nm for **P**2, which has 26 nm red shift with respect to that for **P**1 in DCM. Furthermore, the absorption intensity and the extinction coefficient of **P**2 are bigger than those of **P**1 in DCM. The enhanced absorption intensity and the red-shifted absorption spectrum are displayed for **P**2 instead of **P**1 in their neat films. It indicates that introducing the triphenylamine unit in the side chain of the D-A-based polymers has

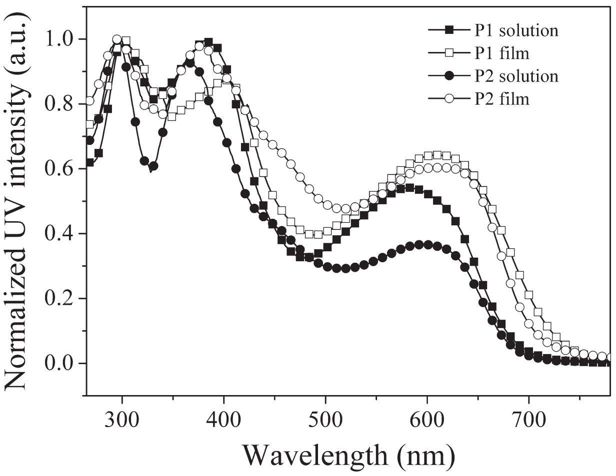

FIGURE 1 Normalized UV-Vis absorption spectra of the P1 and P2 in DCM and their neat films at room temperature.

better effect to improve the absorption properties of its resulting polymers (Fig. 1).

Electrochemical Study

In order to further understand the influence of the pendent groups to the highest occupied molecular orbital (HOMO) and the lowest unoccupied molecular orbital (LUMO) energy levels (E_{HOMO} and E_{LUMO}), the electrochemical behaviors of **P**1 and **P**2 films were investigated by cyclic voltammetry (CV). The resulting CV data are listed in Table 2. The onset oxidation potential (E_{ox}) and reduction potential (E_{red}) were observed in a range of 0.68–0.75 V and −0.85 to −0.87 V versus SCE, respectively. According to the empirical formulas: $E_{\mathrm{HOMO}} = -(E_{\mathrm{ox}} + 4.40)$ eV and $E_{\mathrm{LUMO}} = -(E_{\mathrm{red}} + 4.40)$ eV, the HOMO and LUMO energy levels for these polymers were obtained Finally, the electrochemical band gaps (E_g) of **P**1 and **P**2 were calculated based on the formula of $E_g = E_{\mathrm{LUMO}} - E_{\mathrm{HOMO}}$. It is found that **P**2 has a decreased oxidation potential and reduction potential than **P**1. The E_{HOMO} and E_{LUMO} levels of **P**2 are 0.02 eV and 0.07 eV higher than the corresponding levels of **P**1, respectively. This result indicates that introducing triphenylamine moieties into the side chain of the D-A-based copolymers can further tuning the E_{HOMO} and E_{LUMO} levels for the resulting polymers.

Photovoltaic Properties

As $PC_{71}BM$ has similar electronic properties to $PC_{60}BM$ but a considerably higher absorption coefficient in the visible region, here it was chosen as an electron acceptor instead of $PC_{60}BM$. The photovoltaic performance of these devices is listed in Table 3 at different processing condition. While the blending ratios of polymer and $PC_{71}BM$ were tuned from 1:1 to 1:3, the devices exhibited significantly increased PCE, J_{sc}, and *FF*. After annealed, the resulting devices further presented increased PCE and J_{sc}. The PCE from 1.71% to 3.43% and J_{sc} from 7.59 to 9.20 mAcm^{-2} were observed in the **P**2-based devices with increasing ratios from 1:1 to 1:3 under the annealed condition, when the **P**1-based devices displayed an elevatory PCE from 0.46% to 1.50% and J_{sc} from 2.87 to 7.81 mAcm^{-2} at the same condition, respectively. Therefore, adding ratio of $PC_{71}BM$ and annealing are available to increase the PCE and J_{sc}. As the thermal annealing processes is available to improve the morphology of the active layer greatly, it should result in excellent interpenetrating networks in the active layer and further facilitate charge separation and transportion of photogenerated excitons. Therefore, the devices exhibited higher efficiency under annealing condition. For intuitive comparison, the *J-V* characteristics of the **P**1- and **P**2-based BHJ PSCs are shown in Figure 3 at a blending ratio of 1:3 between polymer and $PC_{71}BM$ under the illumination of AM 1.5 G (100 mW/m^2) from a solar simulator. Obviously, the **P**2-based devices presented better photovoltaic performance than the **P**1-based devices under annealing condition. Incorporating triphenylamine group into the side chain of benzo[1,2-b:4,5-b′] dithiophene-*alt*-2,3-biphenyl quinoxaline copolymer has positive

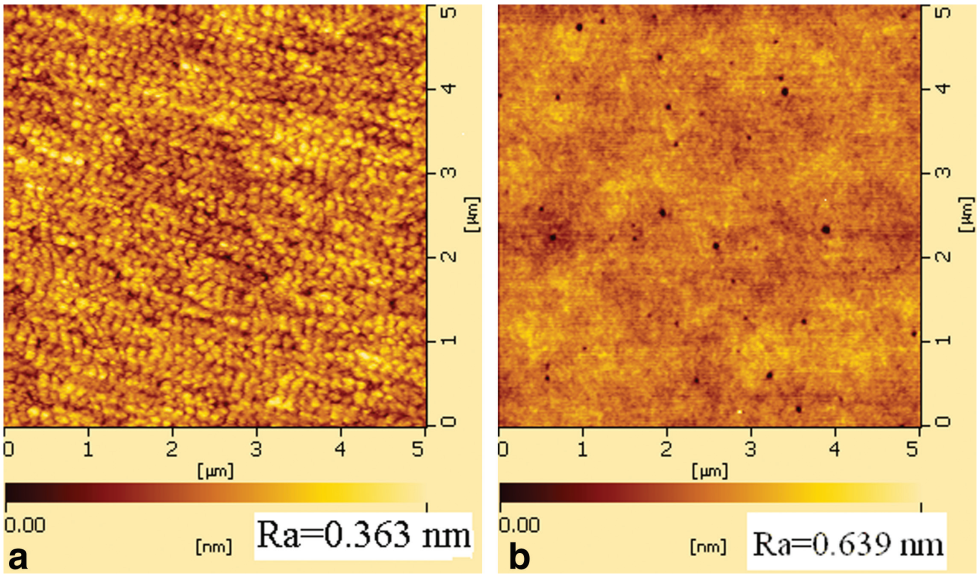

FIGURE 2 Tapping-mode AFM images of the P1 (a) and P2 (b) films on quartz glass.

TABLE 2 Electrochemical Properties of **P**1 and **P**2

Polymer	$E^{red}_{1/2}$ (V)	$E^{ox}_{1/2}$ (V)[a]	E_{HOMO} (eV)[b]	E_{LUMO} (eV)[b]	E_g (eV)[c]	E_{el} (eV)[c]
P1	−0.87	0.68	−5.27	−3.72	1.72	1.65
P2	0.85	0.75	−5.25	−3.65	1.75	1.70

[a] Potential values are reported by cyclic voltammetry.

[b] $E_{LUMO} = -(4.40 + E^{red}_{1/2})$ eV, $E_g = E_{LUMO} - E_{HOMO}$.

[c] Estimated according to the UV-Vis absorption spectra of the polymer films at 298 K.

effect on improving the photovoltaic performance for its resulting polymer in the cells. The highest PCE of 3.43%, a J_{sc} of 9.20 mA cm^{-2}, and a *FF* of 47.0% were obtained in the **P**2-based solar cells at a blending ratio of 1:3.

We noted that the experimental V_{oc} of the P1- and P2-based devices was 0.66 and 0.80 V under this blending ratio, respectively. In general, there is a linear relationship between V_{oc} and the energy gap between the HOMO level of the donor polymer and LUMO level of an acceptor. Based on this rule, the theoretical V_{oc} is estimated to be about 0.95 V (using −4.0 eV for the LUMO energy level of PC$_{71}$BM).[24] Compared to the theoretical V_{oc}, the experimental V_{oc} is reduced and has some deviations of 0.15–0.29 V. The lower experimental V_{oc} is closely related not only to the dark current-voltage curve of the diode but also to the interface interaction between their domains, which influences the charge photogeneration efficiency and recombination.[25,26]

On the other hand, by comparison with the device performance of the previous quinoxaline conjugated polymers-based solar cells,[27] we observed that the **P**2-based cells exhibited significantly increased PCE level, as well as a parallel V_{oc} and J_{sc} values, respectively. However, the *FF* level here was not improved. It is considered that the *FF* value could be improved by using different solvents,[28] adding various additives,[29] and/or using a buffer layer.[30] Hence, to further improve it, some optimized work for the devices need be carried out.

CONCLUSIONS

In summary, two D-A-based benzo[1,2-b:4,5-b']dithiophene-*alt*-2,3-biphenyl quinoxaline copolymers of **P**1 and **P**2 were made with functional thiophene or triphenylamine units in the 4-positions of phenyl rings. The **P**2 copolymer with pendent triphenylamine unit exhibited the best performance in the BHJ PSCs. The maximum PCE of 3.43% with a V_{oc} of 0.80 V and a J_{sc} of 9.20 mA cm^{-2} were achieved in these devices under the illumination of AM 1.5, 100 mW cm^{-2}. Our work indicated that incorporating triphenylamine pendant into the side chain of the D-A-based copolymers can greatly improved the photovoltaic properties for its resulting polymers in the BHJ PSCs.

EXPERIMENTAL

Materials and Measurements

All manipulations were performed under dry nitrogen flow. All reagents were obtained from Aldrich and directly used without further purification. Scheme 1 illustrates the synthetic route of the polymers.

^{1}H and ^{13}C NMR spectra were recorded on a Bruker DRX 400 spectrometer using tetramethylsilane as a reference in deuterated chloroform solution at 298 K. MALDI-TOF mass spectrometric measurements were performed on Bruker Bifiex III MALDI-TOF. Molecular weight was determined using a Waters GPC 2410 in tetrahydrofuran via a calibration curve of polystyrene as standard. UV-Vis absorption spectra were recorded on a HP-8453 UV visible system. CV was carried out on a CHI660A electrochemical work station in a three-electrode cell dipped in a 0.1*M* tetrabutylammonium hexafluorophosphate (Bu$_4$NPF$_6$) solution in acetonitrile under nitrogen protection at a scan rate of 100 mV/s and room temperature. In this three-electrode cell, a platinum rod, platinum wire, and calomel electrode were used as a working electrode, counter electrode, and reference electrode, respectively. The morphology of the polymer/PCBM blend film was investigated by an AFM on a Veeco, DI Multimode NS-3D apparatus in a trapping mode under normal air condition at room temperature. Tributyl(5-octyl- thiophen-2-

TABLE 3 Photovoltaic Properties of **P**1 and **P**2

Polymer	Polymer:PC$_{71}$BM	Thickness (nm)	Annealing	J$_{sc}$ (mA/cm^2)	V$_{oc}$ (V)	PCE$_{max}$ (PCE$_{averag}$) (%)	FF (%)
P1	1:1[a]	80	No	2.63	0.66	0.40 (0.33)	23
	1:1[b]	80	Yes	2.87	0.68	0.46 (0.39)	24
	1:3[a]	80	No	6.19	0.66	1.19 (1.07)	29
	1:3[b]	80	Yes	7.81	0.66	1.50 (1.44)	29
P2	1:1[a]	80	No	6.26	0.76	1.43 (1.26)	30
	1:1[b]	80	Yes	7.59	0.74	1.71 (1.60)	30
	1:3[a]	80	No	7.60	0.80	2.92 (2.67)	48
	1:3[b]	80	Yes	9.20	0.80	3.43 (3.17)	47

[a] Unannealed.

[b] Annealed at 150°C for 15 min.

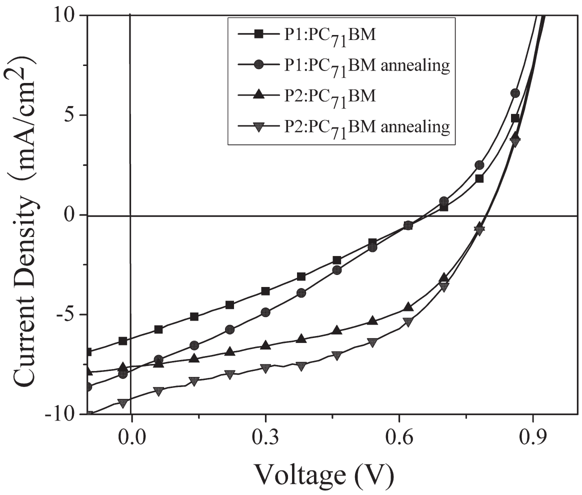

FIGURE 3 *J-V* characteristics of the bulk heterojunction polymeric solar cells with a structure of ITO/PEDOT:PSS/polymer:PC$_{71}$BM (1:3, wt/wt)/LiF/Al under the illumination of AM 1.5 G from a solar simulator (1000 W m^{-2}).

yl)stannane (1), 3,6-dibromobenzene-1,2-diamine, 4-(octyloxy)-N-(4-(octyloxy)phenyl)-N-(4-(4,4,5,5-tetramethyl-1,3,2-dioxaborolan-2-yl)phenyl)benzen amine (3), 2,6-bis(trimethyltin)-4,8-bis(2-ethylhexyloxy)benzo[1,2-b:4,5-b′]dithiophene (M1) were synthesized by the published procedures.[21–23]

Polymer Solar Cell Fabrication and Test

The photovoltaic cells were constructed with a traditional sandwich structure through the following steps. The iridium-tin oxide (ITO)-coated glass substrates were cleaned by a series of ultrasonic treatments for 10 min in acetone, following by deionized water, then 2-propanol. The substrates were dried under a stream of nitrogen and subjected to the treatment of Ar/O$_2$ plasma for 5 min. A filtered aqueous solution of poly(3,4-ethylenedioxy-thiophene)-poly-(styrenesulfonate) (PEDOT:PSS) (Bayer AG) was spun-cast onto the ITO surface at 2000 rpm for 30 s and then baked at 150 °C for 30 min to form a PEDOT:PSS thin film with a thickness of 30 nm. A blend of polymer and PC$_{71}$BM (1:3 wt/wt, 20 mg/mL for polymer) was dissolved in chlorobenzene, filtered through a 0.45-μm poly(tetrafluoroethylene) filter and spun-cast at 3000 rpm for 30 s onto the PEDOT:PSS layer. The substrates were dried under N$_2$ at room temperature and then annealed at 150 °C for 15 min in a nitrogen-filled glovebox. The devices were completed after thermal deposition of a 10-nm lithium fluoride and a 0.5-nm aluminum film as the cathode at a pressure of 6×10^{-4} Pa. The active area was 9 mm^2 for each cell. The thicknesses of the spun-cast films were recorded by a profilometer (Alpha-Step 200, Tencor Instruments).

Device characterization was carried out under an AM 1.5G irradiation with an intensity of 100 mW/cm^2 (Oriel 91160, 300 W) calibrated by a NREL-certified standard silicon cell. Current density-voltage (*J-V*) characteristics were measured by a computer-controlled Keithley 2602 source measurement unit in the dark. All device characterizations were performed under an ambient atmosphere at room temperature.

Synthesis of Materials

Synthesis of M2

A mixture of 2 (0.60 g, 1.00 mmol), 3,6-dibromobenzene-1,2-diamine(0.27 g, 1.00 mmol), solid potassium carbonate, and ethanol (25 mL) was vigorously stirred at 75 °C for 24 h under a nitrogen atmosphere. After cooling, the reaction solution was extracted with dichloromethane and water. The organic layer was collected and dried over magnesium sulfate. The solvent was removed by rotary evaporation and the residue was purified by column chromatography [silica gel, petroleum ether/dichloromethane (5/1) as eluent] to give yellow solid, ^{1}HNMR (400 MHz, CDCl$_3$, ppm): 7.92 (d, $J = 3.6$ Hz, 2H), 7.74 (d, $J = 8.0$ Hz, 4H), 7.69 (d, $J = 8.8$Hz, 4H), 7.31 (d, $J = 3.2$ Hz, 2H), 6.81 (d, $J = 3.0$ Hz, 2H), 2.85-2.82 (t, 4H), 1.73-1.70 (m, 4H), 1.44-1.29 (br, 20H), 0.90 (t, 6H). ^{13}C NMR (CDCl$_3$, 100MHz), δ (ppm): 153.4, 146.8, 140.7, 139.3, 138.1, 136.3, 136.1, 136.0, 133.1, 133.0, 130.8 , 130.2, 129.6, 128.5, 125.3, 125.2, 125.1, 123.7, 123.6, 31.9, 31.6, 30.3, 29.7, 29.3, 29.2, 29.1, 22.7, 14.1.TOF-MS (m/z): Calcd for C$_{44}$H$_{48}$Br$_2$N$_2$S$_2$, 828.2; found, 829.2.

Synthesis of M3

^{1}HNMR (400 MHz, CDCl$_3$, ppm): 7.90 (d, $J = 4.0$ Hz, 2H), 7.75 (d, $J = 8.4$ Hz, 4H), 7.58 (d, $J = 8.8$Hz, 4H), 7.46 (d, $J = 8.0$ Hz, 4H), 7.09 (d, $J = 8.6$ Hz, 8H), 7.00 (d, $J = 8.8$ Hz, 4H), 6.85 (d, $J = 8.4$ Hz, 4H), 3.95-3.92 (t, 8H), 1.81-1.78 (m, 8H), 1.46-1.29 (br, 40H), 0.90 (t, 12H). ^{13}C NMR (CDCl$_3$, 100MHz), δ (ppm): 155.7, 153.8, 148.8, 142.1, 140.6, 139.3, 136.0, 132.9, 131.6, 130.7, 127.5, 126.8, 126.2 , 123.7, 120.4, 115.4, 68.4, 31.8, 29.4, 29.3, 26.1, 22.7, 14.1. TOF-MS (m/z): Calcd for C$_{88}$H$_{102}$Br$_2$N$_4$O$_4$, 1438.6; found, 1438.3.

General Procedures of Stille Coupling Reaction

Taking the preparation of P1 as an example: a mixture of monomers M**1** (77.2 mg, 0.1 mmol), M**2** (82.8 mg, 0.1 mmol), and Pd(PPh$_3$)$_4$ (10 mg) in toluene (4 mL) was degassed with nitrogen flow and stirred at 90 °C for 48 h under nitrogen atmosphere. After cooled to room temperature (RT), tributyl(thiophen-2-yl)stannane (37 mg, 0.10 mmol) was added and the mixture was refluxed for 12 h. Then 2-bromothiophene (32 mg, 0.20 mmol) was injected and the mixture was refluxed for another 12 h. The mixture was cooled to RT and poured into 200 mL MeOH to form precipitate. The precipitate was collected and dissolved in DCM. The filtrate was poured into 200 mL MeOH again to provide precipitate. Then, the precipitate was washed with acetone in a Soxhlet apparatus for 48 h to give P1 as black solid. The polymerization results are summarized in Table 1.

P1: black solid, 90.1mg, yield: 81.1%. ^{1}H NMR (CDCl$_3$, 400 MHz, ppm): 8.26–7.47 (br, 12H), 7.39–7.10 (br, 2H), 6.93–6.70 (br, 2H), 4.45–3.96 (br, 4H), 3.03–2.71 (br, 4H), 1.97–1.17(m, 42H), 1.16–0.59 (br, 18H). ^{13}C NMR (CDCl$_3$, 100MHz), δ (ppm): 152.4, 150.8, 146.3, 144.3, 141.3, 140.2, 138.4, 136.0, 135.3, 133.0, 131.4, 131.2, 130.8 , 130.2, 129.8, 128.3, 127.5, 125.4, 125.2, 125.1, 123.4, 123.1, 40.9, 32.0, 31.7, 30.5, 29.5, 29.3, 29.2, 23.2, 22.7, 14.1. Mn=1.61×10^4 g mol^{-1}; Mw=3.29×10^4 g mol^{-1}; PDI=2.04.

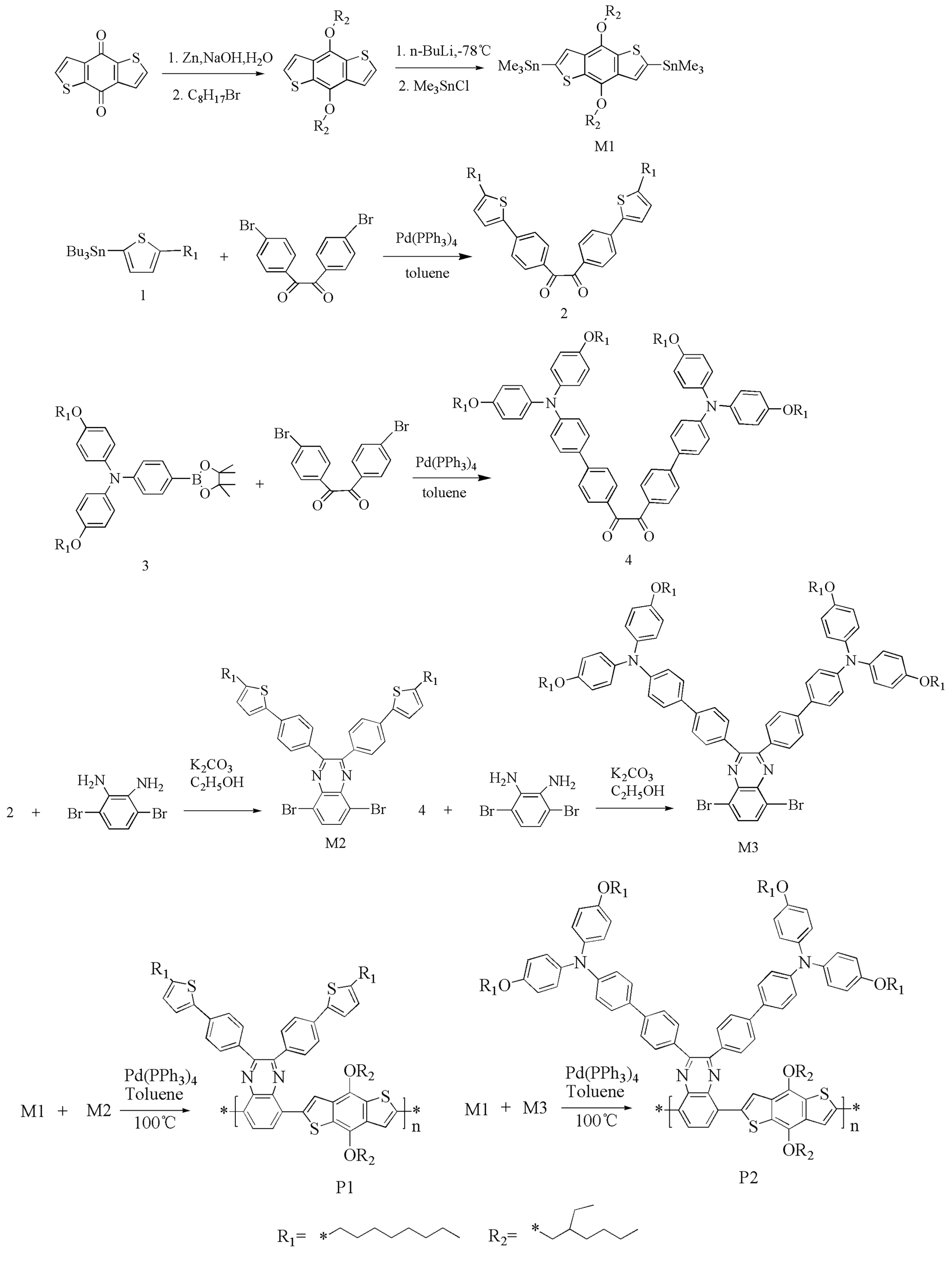

SCHEME 1 Synthesis of the P1 and P2 by the Stille cross-coupling reaction.

P2: black solid, 152.3mg, yield: 88.3%. ^{1}H NMR ($CDCl_3$, 400 MHz, ppm): 8.22–7.81 (br, 24H), 7.80–7.24 (d, J = 7.0 Hz, 2H), 7.21–6.93 (d, J = 8.0 Hz, 6H), 6.92–6.70 (d, J = 8.0 Hz, 6H), 4.07–3.79 (br, 8H), 3.61–3.43 (br, 4H), 2.03 (t, 12H), 1.67–1.08 (br, 60H), 1.07–0.53 (br, 18H). ^{13}C NMR ($CDCl_3$, 100MHz), δ (ppm): 155.5, 148.5, 144.3, 140.7, 139.1, 138.9, 137.5, 137.0, 136.8, 132.4, 132.1, 131.5, 130.9, 130.8, 127.3, 126.6, 126.0, 123.7, 120.8, 115.4, 68.3, 31.9, 30.6, 29.5, 29.3, 26.2, 22.7, 14.3, 14.1. Mn=2.73 × 10^4 g mol^{-1}; Mw=5.34 × 10^4 g mol^{-1}; PDI=1.96.

ACKNOWLEDGMENTS

Thanks to the financial supports from the National Natural Science Foundation of China (Grant Nos. 21172187, 91233112 and 50973093), the Innovation Group and Xiangtan Joint

Project in Hunan Natural Science Foundation (Grant Nos. 12JJ7002 and 12JJ8001), the Specialized Research Fund for the Doctoral Program of Higher Education (Grant No. 2009 430111 0004), the Scientific Research Fund of Hunan Provincial Education Department (Grant Nos. 10A119, 11CY023, and 10B112), and the Postgraduate Science Foundation for Innovation in Hunan Province (Grant No. CX2011B263), Hunan College Students Study and Innovation Experimental Program (2011 and 2012).

REFERENCES AND NOTES

1 H. X. Zhou, L. Q. Yang, A. C. Stuart, S. C. Price, S. B. Liu, W. You, *Angew. Chem. Int. Ed.* **2011,** *50*, 2995–2998.

2 A. Facchetti, *Chem. Mater.* **2011,** *23*, 733–758.

3 C. L. Chochos, S. A. Choulis, **2011, 36, 1326–1414.**

4 Y.-J. Cheng, C.-H. Chen, Y.-S. Lin, C.-Y. Chang, C.-S. Hsu, *Chem. Mater.* **2011,** *23*, 5068–5075.

5 H. J. Son, W. Wang, T. Xu, Y. Y. Liang, Y. Wu, G. Li, L. P. Yu, *J. Am. Chem. Soc.* **2011,** *133*, 1885–1894.

6 W. Y. Nie, C. M. MacNeill, Y. Li, R. E. Noftle, D. L. Carroll, R. C. Coffin, *Macromol. Rapid Commun.* **2011,** *32*, 1163–1168.

7 C. H. Duan, X. W. Hu, K.-S. Chen, H.-L. Yip, W. Li, F. Huang, A. K.-Y. Jen, Y. Cao, *Sol. Energy Mater. Sol. Cells* **2012,** *97*, 50–58.

8 Z. L. Wu, B. H. Fan, A. Y. Li, F. Xue, J. Y. Ouyang, *Org. Electron.* **2011,** *12*, 993–1002.

9 Z. C. He, C. M. Zhong, S. J. Su, M. Xu, H. B. Wu, Y. Cao, *Nat. Photon*. **2012,** *6*, 591–595.

10 W. L. Ma, C. Y. Yang, X. Gong, K. Lee, A. Heeger, *J. Adv Funct Mater.* **2005,** *15*, 1617–1622.

11 G. Li, V. Shrotriya, J. Huang, Y. Yao, T. Moriarty, K. Emery, Y. Yang, *Nat. Mater.* **2005,** *4*, 864–868.

12 J. Min, Z.-G. Zhang, S. Y. Zhang, M. J. Zhang, J. Zhang, Y. F. Li, *Macromolecules* **2011,** *44*, 7632–7638.

13 C.-H. Chen, C.-H. Hsieh, M. Dubosc, Y.-J. Cheng, C.-S. Hsu, *Macromolecules* **2010,** *43*, 697–708.

14 D. Patra, D. Sahu, H. Padhy, D. Kekuda, C.-W. Chu, H.-C. Lin, *J. Polym. Sci. Part A: Polym. Chem.* **2010,** *48*, 5479–5489.

15 J. E. Carle, M. Jørgensen, M. Manceau, M. Helgesen, O. Hagemann, R. Søndergaard, *Sol. Energy Mater. Sol. Cells* **2011,** *95*, 3222–3226.

16 J. Li, X. P. Deng, Z. Y. Zhang, Y. F. Wang, Y. Liu, K. Q. He, Y. Huang, Q. Tao, L. X. Quan, W. G. Zhu, *J. Polym. Sci. Part A: Polym. Chem.* **2012,** *50*, 4686–4694.

17 L. J. Huo, Z. Tan, X. Wang, Y. Zhou, M. F. Han, Y. F. Li, *J. Polym. Sci. Part A: Polym. Chem.* **2008,** *46*, 4038–4049.

18 Q. Peng, J. Xu, W. X. Zheng, *J. Polym. Sci. Part A: Polym. Chem.* **2009,** *47*, 3399–3408.

19 E. G. Wang, L. T. Hou, Z. Q. Wang, Z. F. Ma, S. Hellstrom, W. L. Zhuang, F. L. Zhang, O. Inganas, M. R. Andersson, *Macromolecules* **2011,** *44*, 2067–2073.

20 J. Zhang, W. Z. Cai, F. Huang, E. G. Wang, C. M. Zhong, S. J. Liu, M. Wang, C. H. Duan, T. B. Yang, Y. Cao, *Macromolecules* **2011,** *44*, 894–901.

21 Y.-L. Yang, Y.-H. Lee, C.-J. Chang, A.-J. Lu, W.-C. Hsu, L. Y. Wang, M.-K. Leung, C.-A. Dai, *J. Polym. Sci. Part A: Polym. Chem.* **2010,** *48*, 1607–1616.

22 P.-I. Lee, S. L.-C. Hsu, J. F. Lee, H.-Y. Chuang, P. Y. Lin, *J. Polym. Sci. Part A: Polym. Chem..* **2011,** *49*, 662–670.

23 R. M. Duan, L. Ye, X. Guo, Y. Huang, P. Wang, S. Q. Zhang, J. P. Zhang, L. J. Huo, J. H. Hou, *Macromolecules* **2012,** *45*, 3032–3038.

24 B. Walker, A. B. Tamayo, X.-D. Dang, P. Zalar, J. H. Seo, A. Garcia, M. Tantiwiwat, T.-Q. Nguyen, *Adv. Funct. Mater.* **2009,** *19*, 3063–3069.

25 M. C. Scharber, D. Mühlbacher, M. Koppe, P. Denk, C. Waldauf, A. J. Heeger, C. J. Brabec, *Adv. Mater.* **2006** *18*, 789–794.

26 S. Yamamoto, A. Orimo, H. Ohkita, H. Benten, S. Ito, *Adv. Energy Mater.* **2012,** *2*, 229–237.

27 J. Y. Zou, H.-L. Yip, Y. Zhang, Y. Gao, S.-C. Chien, K. O'Malley, C.-C. Chueh, H. Z. Chen, A. K. Jen, *Adv. Funct. Mater.* **2012,** *22*, 2804–2811.

28 B. Walker, A. Tamayo, D. T. Duong, X.-D. Dang, C. Kim, J. Granstrom, T.-Q. Nguyen, *Adv. Energy Mater.* **2011,** *1*, 221–229.

29 J. K. Lee, W. L. Ma, C. J. Brabec, J. Yuen, J. S. Moon, J. Y. Kim, K. Lee, G. C. Bazan, A. J. Heeger, *J. Am. Chem. Soc.* **2008,** *130*, 3619–3623.

30 Z. C. He, C. Zhong, X. F. Xu, L. J. Zhang, L. Huang, J. W. Chen, H. B. Wu, Y. Cao, *Adv. Mater.* **2011,** *23*, 3086–3089.